DOI: 10.1002/chem.201301011

Single-Step Microwave-Mediated Syntheses of Oxazoles and Thiazoles from 3-Oxetanone: A Synthetic and Computational Study

David Orr,[a] Alexandra Tolfrey,[a] Jonathan M. Percy,*[a] Joanna Frieman,[a] Zoë A. Harrison,*[b] Matthew Campbell-Crawford,[c] and Vipulkumar K. Patel[b]

Abstract: The direct microwave-mediated condensation between 3-oxetanone and primary amides and thioamides has delivered moderate to good yields of (hydroxymethyl)oxazoles and (hydroxymethyl)thiazoles. The reactions use a sustainable solvent and only require short reaction times. These are highly competitive methods for the construction of two classes of valuable heteroarenes, which bear a useful locus for further elaboration. Electronic structure calculations have shown that the order of events involves chalcogen atom attack at sp^3 carbon and alkyl–oxygen cleavage. The critical role of acid catalysis was shown clearly, and the importance of acid strength was demonstrated. The calculated barriers were also fully consistent with the observed order of thioamide and amide reactivity. Spontaneous ring opening involves a modest degree of C–O cleavage, moderating the extent of strain relief. On the acid-catalysed pathway, C–O cleavage is less extensive still, but proton transfer to the nucleofuge is well advanced with the carboxylic acid catalysts, and essentially complete with methanesulfonic acid.

Keywords: annulation · density functional calculations · microwave chemistry · nitrogen heterocycles · sulfur heterocycles

Introduction

Oxetanes are rapidly becoming an important part of the repertoire of the medicinal chemist, because of the ability of these heterocycles to mimic ketonic carbonyl groups and *gem*-dimethylated sp^3 centres.[1] Methods for the introduction of the oxetanyl motif are becoming more developed[2] and there is a growing array of procedures that allow the complete oxetane unit to be introduced.[3] However, oxetane derivatives may also be interesting synthetic building blocks for the construction of other heterocycles. There are relatively few examples of oxetane ring-opening reactions in the literature, but recently, Carreira and co-workers[4] showed how isoxazoles **2** could be formed in a sequence begun by the reaction of the conjugate base of a nitroalkane with 3-oxetanone (**1**; Scheme 1). The heterocyclic ketone **1** is now commercially available and, while it is relatively expensive, its latent reactivity in strain-relieving ring opening makes it a very interesting species for further exploration.

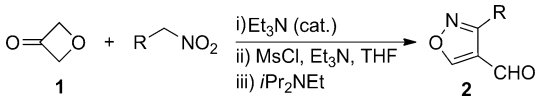

Scheme 1. Carreira and co-workers' isoxazole synthesis from 3-oxetanone begins with a Henry reaction and features a pivotal ring opening through an oxete intermediate.

During the course of the synthesis of a drug lead, we discovered trace amounts of an oxazole product when a benzamide was condensed with **1** under acidic conditions (acetic acid/sulfamic acid). Oxazoles and the related thiazoles occur widely in natural products, including species in which they are linked, and in some drug leads. Figure 1 shows a number of natural products that contain these heteroarenes. Virginiamycin M1 (**3**) is used to treat resistant bacterial infections,[5] (−)-Mycothiazole (**4**) is a marine natural product with cytotoxicity against lung cancer cells,[6] while Bistratamide C (**5**) is one of the *Lissoclinum* cyclopeptides, a class of cyctotoxic agents from marine Ascidians.[7] There has been considerable recent interest in the synthesis of these heteroarenes[8] reflecting their frequent occurrence, prompting us to explore our serendipitous finding to see if a useful synthetic method could be discovered. It has also provided an opportunity to explore some of the mechanisms available for oxetanone ring opening, a process that has not been explored to our knowledge, apart from in a preliminary manner by Carreira and co-workers.

[a] D. Orr, A. Tolfrey, Prof. Dr. J. M. Percy, J. Frieman
WestCHEM Department of Pure and Applied Chemistry
University of Strathclyde, Thomas Graham Building
295 Cathedral Street, Glasgow G1 1XL (UK)
Fax: (+44) 0141-548-4822
E-mail: jonathan.percy@strath.ac.uk

[b] Z. A. Harrison, Dr. V. K. Patel
Refractory Respiratory Inflammation DPU
GlaxoSmithKline Medicines Research Centre
Gunnels Wood Road, Stevenage SG1 2NY (UK)
Fax: (+44) 01438 768302
E-mail: zoe.x.harrison@gask.com

[c] M. Campbell-Crawford
Fibrosis DPU, GlaxoSmithKline Medicines Research Centre
Gunnels Wood Road, Stevenage SG1 2NY (UK)

Supporting information for this article is available on the WWW under http://dx.doi.org/10.1002/chem.201301011.

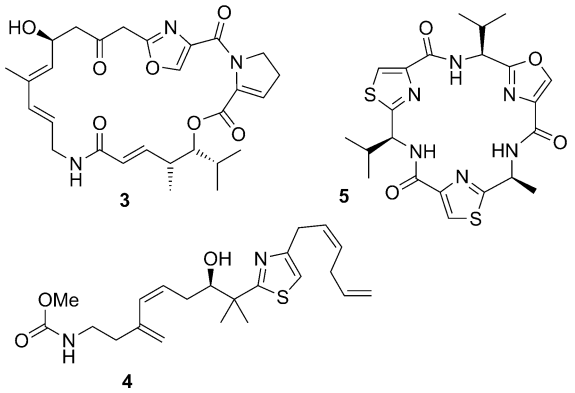

Figure 1. Oxazole- and thiazole-containing natural products.

Table 1. First-generation microwave-mediated azole syntheses in trifluoroacetic acid/acetic acid mixtures.

Amide or thioamide	X	Product	Method[a,b]	T [°C]	Time [h]	Yield [%][c]
6a, R = Ph	O	**8a**	A	120	3.5	47[d]
			B	80	28	48
6b, E-PhHC=CH	O	**8b**	A	120	2.5	60
			B	80	51	52
6c, 2-thiophenyl	O	**8c**	A	120	2.5	50
			B	80	52	68[e]
6d, cyclohexyl	O	**8d**	A	120	3.0	21
			B	80	192	31[f]
7a, Ph	S	**9a**	A	85	3.5	52

[a] Method A: microwave heating. [b] Method B: conventional heating. [c] All reactions were carried out on 1–2 mmol scale at 120 °C. [d] 10 mmol scale, 120 °C. [e] Crude GC/MS yield. [f] Crude yield.

Results and Discussion

To optimise our use of costly 3-oxetanone, we fixed the initial stoichiometry for the reaction with benzamide at 1:1 and retained acetic acid as the solvent, because it is inexpensive, polar and sustainable.[9] A reaction screen was carried out on a 0.5 mmol scale in the microwave; the parameters varied were temperature (80–140 °C), time (20–300 min), stronger acid catalyst (none, sulfamic acid, trifluoroacetic acid, and HCl, generated in situ from tetramethylsilyl chloride), equivalents of stronger acid (0.1–0.5 equivalents) and reaction concentration (0.4–2.1 M). Reactions that achieved the highest conversions of benzamide with the lowest levels of side-product formation (assayed by GC-MS) were selected for further investigation. The following generalities emerged; a stronger acid catalyst was essential (or the reaction was very slow) and trifluoroacetic acid was the most effective of the three used in the initial screen (Scheme 2).

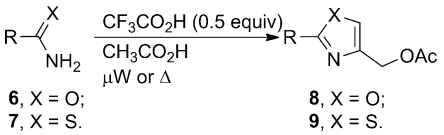

Scheme 2. First-generation microwave-mediated azole syntheses in trifluoroacetic acid/acetic acid mixtures.

A high loading of catalyst (0.5 equivalents) was required and the combination of a reaction temperature of 120 °C and concentration of 0.4 M gave high (>95 %) conversion of the amide and consistent results. Acetates **8a–c** were prepared in good (47–60 %) yields under these conditions (Table 1); cyclohexyl congener **8d** reacted less successfully (21 % isolated yield at full conversion). Thiazolyl analogue **9a** (52 %) was also prepared from commercial thiobenzamide. The mass balance in these reactions is unfortunately accounted for by tar formation; in some cases, traces of the corresponding trifluoroacetate esters were detected in the crude products by GC-MS, but we were unable to isolate them. We tried dividing the total microwave irradiation time into a series of short pulses as described by Ley and coworkers,[10] but there was no improvement in isolated yield (20 min periods of heating at 120 °C, followed by 10 min rest periods).

Conventional heating at 80 °C could also be used to prepare **8a–d**; yields were comparable though a very long reaction time was required for **8d**. These results were pleasing, but the products would have more value if the free hydroxyl group was available for oxidation to the aldehyde or other manipulation without the need for an ester cleavage. Another reaction solvent that could not act as an acetyl donor was clearly required and we selected dimethyl carbonate, which has a lower dielectric constant ($\varepsilon_S = 3.1$)[11] than acetic acid ($\varepsilon_S = 6.2$). Solvents with such low dielectric constants do not usually respond strongly to microwave heating,[12] but dimethyl carbonate has good solvent characteristics for scale-up and sustainable synthesis,[13] and some promise as a sustainable methylating agent.[14] A range of acids were deployed including trifluoroacetic, oxalic, sulfamic, methanesulfonic and *p*-toluenesulfonic acids; the effective combination emerging from the screen was methanesulfonic acid in DMC. There was no correlation between acid strength and performance; the relevant pK_a values are TsOH (pK_a −2.8),[15a] MsOH (pK_a −1.9),[15a] TFA (pK_a 0.23),[15b] H_2NSO_3H (pK_a 1.0),[15c] oxalic acid (pK_a 1.23),[15d] and acetic acid (pK_a 4.76)[15d] so the most effective acid was neither the strongest nor the weakest.[15] Scheme 3 shows the best conditions discovered from a screen; the yields of free (oxazolyl)-methyl alcohols were lower than those of the acetates, but are still acceptable given the directness and simplicity of the synthetic procedures. Crystals of sufficiently high quality to allow analysis by X-ray diffraction were grown for alcohol **10a**, confirming its structure. However, the method is much

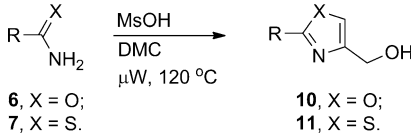

Scheme 3. Second-generation microwave-mediated oxazole and thiazole syntheses in methanesulfonic acid/dimethyl carbonate mixtures.

more effective for thiazole synthesis. A higher (54%) yield of thiazole **11a** was obtained under these conditions, and a change in reaction stoichiometry to use a 50% molar excess of thioamide increased the yield further to 64% (with thioamide recovery possible). Unfortunately, this tactic was not effective for oxazole synthesis because the amides and oxazole products often had very similar R_F values, making chromatographic purification very difficult.

A range of primary thioamides[16] was prepared (see the Supporting Information for details) using the extremely convenient microwave method of Perlmutter and co-workers,[17] which exposes the primary amides (we held a stock of these compounds) to diphosphorus pentasulfide supported on alumina; Table 2 summarises the results obtained to date and makes clear the efficacy of this approach for thiazole synthesis.

Table 2. Second-generation microwave-mediated azole syntheses in methanesulfonic acid/dimethyl carbonate mixtures.

R	Amide	X=O	Yield [%]	Thioamide	X=S	Yield [%][a]
Ph	**6a**	**10a**	36	**7a**	**11a**	64
E-PhHC=CH	**6b**	**10b**	24	**7b**	**11b**	44
2-thiophenyl	**6c**	**10c**	22	**7c**	**11c**	50[b]
cyclohexyl	**6d**	**10d**	17	**7d**	**11d**	63
(3-MeO)Ph	**6e**	n.d.	n.d.	**7e**	**11e**	47[b]
(4-MeO)Ph	**6f**	**10f**	15	**7f**	**11f**	50
(4-Br)Ph	**6g**	**10g**	13	**7g**	**11g**	37
(3-F_3C)Ph	**6h**	**10h**	24	**7h**	**11h**	36
*t*Bu	**6i**	**10i**	14	**7i**	**11i**	40[b]
(2-Cl)Ph	**6j**	–	–[c]	**7j**	**11j**	41
(2-Me)Ph	**6k**	–	–	**7k**	**11k**	48

[a] All yields were obtained with 1.5 equivalents of thioamide unless stated otherwise. [b] In this case, a better yield was obtained with 1.0 equivalent of thioamide; the use of an excess resulted in yield loss in mixed fractions in the chromatography. [c] Reaction attempted for 4 h with incomplete conversion.

A range of aromatic substituents were tolerated as were secondary and tertiary alkyl groups; the *E*-cinnamyl group also survived the reaction conditions. There were no trends between substituent character and reaction yield; the main factor determining the yield was the ease of separation of heteroarene product from unreacted amide or thioamide. Literature routes that build thiazoles with this 2,4-disubstitution pattern include Hantzsch syntheses[18] (thioamide condensations with pyruvate-type electrophiles), and thiazoline oxidation[19] or bromination/dehydrobromination[20] procedures. Our procedure is extremely competitive because of its directness and high atom-efficiency.

There is very little mechanistic work on oxetane or oxetanone ring-opening in the literature. Oxetane, the parent heterocycle for the synthetic building block used in this study, is a strained cyclic ether; opening of this ring[21] releases a significant strain energy of 25.5 kcal mol^{-1} according to experiment[22] and theory.[23] However, ring-opening reactions must overcome a high kinetic barrier; Banks evaluated $\Delta G^{\neq}$ (gas phase) at 58.4 kcal mol^{-1} for the ring-opening reaction with ammonia (MP2(Full)/6-311++G(d,p)//MP2(Full)/6-31+G*). We have used electronic structure calculations to examine a range of possible ring-opening modes and attempt to gain insight into the reaction mechanism. Because of the high kinetic cost of opening the ring, we assume that locating the lowest energy transition structure which involves C–O scission will reveal the most favoured mode of ring opening and that mapping the entire energy surface will provide no additional insights.

Initial structures were obtained at the RI-MP2/6-31G* level of theory, then reoptimised (MP2/6-31+G*) with full frequency calculations, implemented in Spartan'08.[24] Transition structure **12a** (Figure 2) reported by Banks was reproduced by an MP2/6-31+G* geometry optimisation; $\Delta G^{\neq}$ (gas phase) calculated by this method was 59.8 kcal mol^{-1}, which is in excellent agreement with the published value and instils confidence that the use of the much smaller basis will deliver useful results. Carriera and co-workers used a different level of theory (B3LYP/6-311G(d,p), or 6-311G**) to interrogate aspects of the isoxazole-forming reaction of Scheme 1. Because the implementation of this method is more economical with Spartan'08, we also examined all the key reactions using this additional level of theory. The use of the B3LYP functional has been subject to criticism in recent years, but Goodman[25] has provided evidence of its effectiveness for dealing with transition states of reactions of small organic molecules, and of its relatively low degree of vulnerability to the integration grid errors attributed[26] to the Q-CHEM grid used by the Spartan programmes.

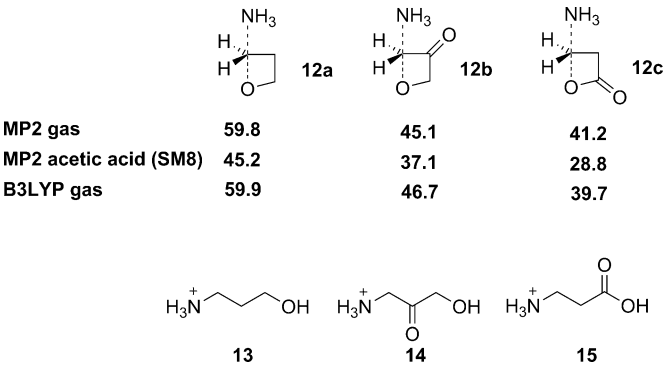

Figure 2. Calculated $\Delta G^{\neq}$ (kcal mol^{-1}, 298 K) for nucleophilic ring opening of oxetane, 3-oxetanone and 2-oxetanone with ammonia, (MP2/6-31+G* and B3LYP/6-311+G**) and the products of ring opening used to evaluate leaving group pK_a.

We did not expect that the presence of the carbonyl group in 3-oxetanone would lower the barrier to C–O scission significantly; while nucleophilic substitution next to a carbonyl group is usually accelerated,[27] the scissile σ-bond and the relevant carbonyl group orbital would be expected to be orthogonal[28] if the oxetanone ring was planar. However, the barrier to oxetane ring opening is considerably lower at 45.1 kcal mol^{-1}, predicting that the ring-opening reaction of 3-oxetanone with ammonia would be 10^{11} times

faster than the reaction of oxetane itself. The products of ring opening are **13** and **14** and their hydroxyl group pK_a values (in water at 298 K, calculated using ACD/Labs software within CAS SciFinder) are 14.95 and 12.94, so it is clear that lower nucleofuge basicity alone cannot be responsible for the higher reactivity of 3-oxetanone. A decrease in leaving group basicity of 2 pK_a units and a Brønsted β_L of −1.0 predicts only a 100-fold increase in reactivity. In the transition structures **12a** and **b**, the ring is twisted, resembling the puckered conformation of cyclobutane; in the 3-oxetanone structure **12b**, the C=O bond sits at approximately 45° to the forming C–N bond. This twisting distorts the O-C-N angle to 164° (from 175.5° in **12a**) and **12b** is slightly earlier with respect to C–N bond formation (C–N is 1.83 compared to 1.76 Å in **12a**). The location of the carbonyl group suggests strongly that some degree of transition state stabilisation is being achieved by the C=O group. The C2–C3 bond length changes from 1.53 to 1.48 Å between **1** and transition structure **12b**, consistent with the development of some partial double bond character between the two carbons at the transition state. The $\Delta G^{\neq}$ (gas phase) value calculated for **12c** is lower still at 41.2 kcal mol^{-1}, and the atoms of the opening ring are coplanar, with C–O and C–N distances similar to those for **12a**; in this case, the calculated carboxylate pK_a is 3.65. Scheme 4 shows the ring opening of

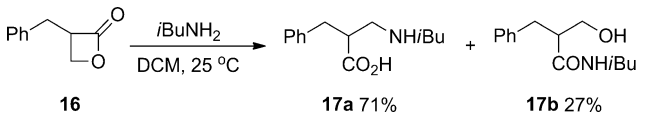

16 **17a** 71% **17b** 27%

Scheme 4. Competitive acyl and alkyl C–O cleavage modes for 2-oxetanone derivative **16**.

16 by benzylamine in dichloromethane; this reaction involves competitive acyl and alkyl C–O cleavage to afford **17a** and **b** respectively under mild conditions,[29] and suggests very strongly that a calculated barrier of 40 kcal mol^{-1} in the gas phase corresponds to a cleavage reaction, which can occur readily in solution under relatively mild conditions.

Amides are significantly less nucleophilic than ammonia so we examined a wider set of reactions related to the ring opening of **1**; however, simple intermolecular reactions lead to the lowest energy barriers (Table 3) via transition structures of types **18** or **19** (Figure 3; a wider set of ring-opening reactions is described fully in the Supporting Information).

The barrier $\Delta G^{\neq}$ calculated for the ring opening of **1** with model amide formamide (O-attack) rose to 49.3 kcal mol^{-1} from the lower value (45.1 kcal mol^{-1}) for the more nucleophilic ammonia. A higher barrier (59.1 kcal mol^{-1}) was calculated for formamide N-attack while S-attack for thioformamide (41.4 kcal mol^{-1}) via **18b** was the most favourable pathway. All the modes of intermolecular attack involved N–H···O=C hydrogen-bond formation; these interactions formed during the optimisation even when the two functional groups were initially remote. The intermolecular O-attack

Table 3. Free-energy barriers ($\Delta G^{\neq}$, kcal mol^{-1}, 298 K) calculated for opening of 3-oxetanone **1** for nucleophilic O- and S-attack by amides and thioamides transition structures **19a–h** and **20**.

Structure	R^1	X	R^2	MP2/gas[a]	MP2/acetic acid[a]	B3LYP/gas[b]
18a	–	O	–	49.3	47.1	51.7
18b	–	S	–	41.4	40.4	43.2
19a	H	O	CH_3	35.8	38.7	38.0
19b	H	S	CH_3	31.4	34.2	35.5
19c	H	O	CF_3	26.7	29.0	31.2
19d	H	S	CF_3	24.0	27.5	27.1
19e	Ph	O	CH_3	33.7	–	37.7
19f	Ph	S	CH_3	30.2	–	34.3
19g	Ph	O	CF_3	23.2	–	30.7
19h	Ph	S	CF_3	22.5	–	29.0
20	–			21.2	–	–

[a] (MP2/6-31+G*) gas phase and [SM8]. [b] (B3LYP/6-311+G**).

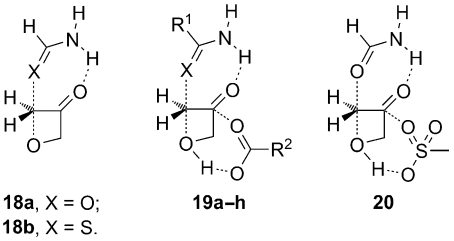

Figure 3. Spontaneous and acid-catalysed transition structure types for opening of 3-oxetanone **1** through nucleophilic O- and S-attack by amides and thioamides.

mode of ring-opening was therefore examined further. A molecule of acetic acid or trifluoroacetic acid was placed so that the acid O–H proton was within approximately hydrogen bonding distance of the oxetanyl oxygen, and optimisation was carried out without constraint. Allowing the optimisation to find the best position for the proton should accommodate both general and specific acid catalysis. Various changes occurred during the optimisation, including flattening of the oxetanyl ring, turning of the attacking amide to hydrogen bond to the acetic acid molecule and partial proton transfer to the oxetanyl oxygen (see the Supporting Information for graphical representations of the transition structures and an overlay).

With the acetic acid molecule present in **19a** (Figure 4b), $\Delta G^{\neq}$ fell to 35.8 kcal mol^{-1} (gas phase). The lower $\Delta G^{\neq}$ value for this reaction is remarkable given the high entropic cost of termolecular reactions compared to their bimolecular counterparts.[30]

The C2–C3 distance is longer when the acetic acid is present and the natural charge on the carbonyl oxygen is lower (−0.479) compared to the structure in the absence of the acetic acid (−0.689); these differences are consistent with an interaction between the substitution centre and the carbonyl group in **18a**; once the acetic acid is present in **19a**, strong stabilisation of the developing charge on the leaving group can occur and the need for ring twisting is relieved. With trifluoroacetic acid posed near the oxetanyl oxygen, the energy for opening by formamide fell still further to

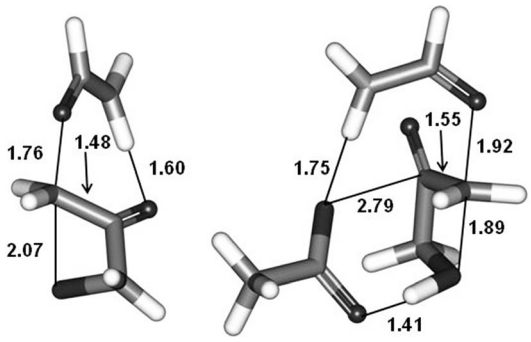

Figure 4. Optimised (gas phase, MP2/6-31+G*) transition structures for a) 3-oxetanone opening with formamide **18a**; b) 3-oxetanone opening with formamide in the presence of acetic acid **19a**. Distances are shown in Å.

26.7 kcal mol^{-1} (gas phase), consistent with the significantly higher acidity of trifluoroacetic acid (the pK_a values of trifluoroacetic acid and acetic acid are 0.23 and 4.76 respectively, vide infra). With thioformamide as the nucleophile and trifluoroacetic acid as the catalyst, the barrier fell to 24 kcal mol^{-1} (gas phase), while for formamide in the presence of methanesulfonic acid (pK_a −1.9), $\Delta G^{\ddagger}$ fell further still to 21.2 kcal mol^{-1} (gas phase). Transition structures were reoptimised (MP2/6-31+G*) using Cramer and Truhlar's SM8 method[31] specifying acetic acid as the reaction solvent; unfortunately, a full range of parameters are not available for dimethyl carbonate or related species, so while we can treat the initial reaction conditions (acetic acid/trifluoroacetic acid), the second generation method cannot be dealt with using this solvation treatment. As expected, lower values of $\Delta G^{\ddagger}$ were obtained using the SM8 method (by 14.6, 8.0 and 12.4 kcal mol^{-1} for **12a**, **b** and **c** respectively), but structural differences between gas phase and solution structures were minimal. Intermolecular transition structures **18a** and **b** were slightly lower in (free) energy in acetic acid, but the barriers calculated for **19a–d** were all slightly higher in acetic acid. To gain some insight into this behaviour, we compared the dipole moments of complex **21** (D = 4.14 debye), obtained by relaxing transition structure **19a**, with transition structure **19a** itself (D = 4.18 debye) (Figure 5). There was no significant change in dipole moment on progression to the transition structure, consistent with the absence of a strong transition state stabilising effect in acetic acid. Finally, selected calculations were carried out with the full benzamide or thiobenzamide nucleophiles (**19e–h**) reproducing the trends observed for the formamide and thioformamide models.

The optimised structures from the gas phase calculations were used to quantify approximately the extent of C–O cleavage in the spontaneous and catalysed reactions. The sum of the carbon and oxygen van der Waals radii was used as an estimate of full C–O cleavage and the extension of the C–O bond relative to the oxetanone C–O bond length was used to calculate the percentage extension. A similar approach was used to quantify the extent of O–H formation. In the spontaneous ring opening with ammonia and formamide, C–O cleavage approaches 30%, indicating that the release of ring strain will be modest at the transition state. On the acid catalysed pathway, C–O cleavage is less well advanced at approximately 20%, whereas proton transfer to the oxetanyl oxygen is well advanced (approximately 90%) at the transition state with proton movement involved in the imaginary frequency, whereas proton transfer was complete with the stronger methanesulfonic acid. The two pathways are represented in the More–O'Ferrall–Jencks[32] diagram of Figure 6. After ring opening, a sequence of conventional steps is proposed for oxazole or thiazole formation, summarised in Scheme 5 for **10a** with acetic acid catalysis.

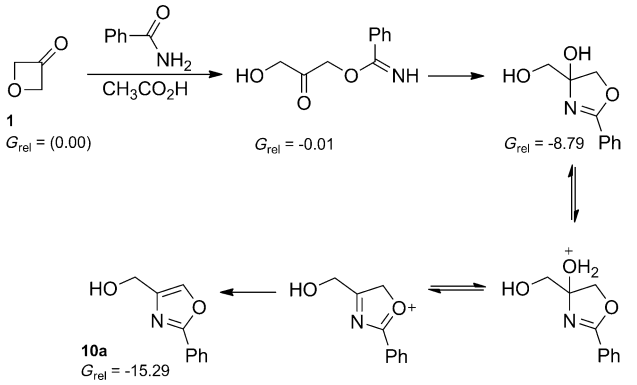

Scheme 5. Intermediates on the pathway to oxazole product **10a** and their free energies (kcal mol^{-1}, 298 K, MP2/6-31+G*).

Overall, the sequence is strongly exergonic, consistent with strain relief and the formation of an aromatic product.

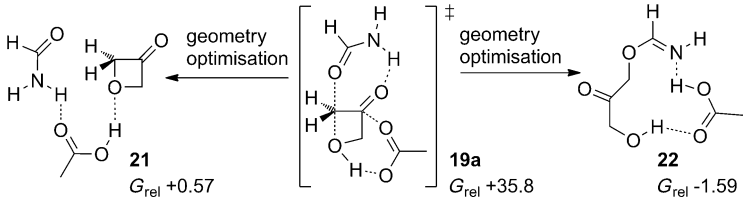

Figure 5. Structures used to calculate dipole moment changes during ring opening of **1** by formamide (gas phase). Free energies (G_{rel}/kcal mol^{-1}) are calculated relative to **1**, formamide and acetic acid as separate molecules.

Conclusion

The direct microwave-mediated condensation between 3-oxetanone and primary amides and thioamides has delivered moderate to good yields of (hydroxymethyl)oxazoles and (hydroxymethyl)thiazoles. The reactions use a sustainable solvent and require only short reaction times. These are highly competitive methods for the construction of two classes of valuable heteroarenes, which bear a useful locus for further elaboration.

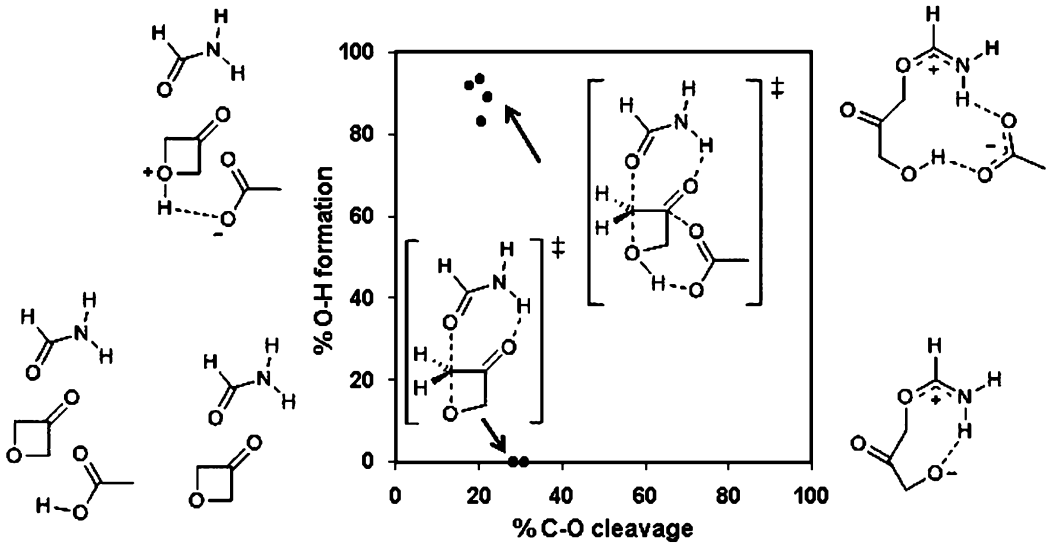

Figure 6. More–O'Ferrall–Jencks diagram showing spontaneous and acid-catalysed oxetanone ring-opening reactions. The bottom right-hand structure is unstable with respect to proton transfer from cationic N to anionic O.

Electronic structure calculations have shown that the order of events involves chalcogen atom attack at sp^3 carbon and alkyl–oxygen cleavage; the favoured termolecular mode of ring opening revealed by the computational study was unexpected. The critical role of acid catalysis was shown clearly, and the importance of acid strength was demonstrated. The calculated barriers were also fully consistent with the observed order of thioamide and amide reactivities. Spontaneous ring opening involves a modest degree of C–O cleavage, moderating the extent of strain relief. On the acid-catalysed pathway, C–O cleavage is less extensive still, but proton transfer to the nucleofuge is well advanced with the carboxylic acid catalysts, and essentially complete with methanesulfonic acid.

Experimental Section

General: NMR spectra were recorded on Bruker DPX-400 or Avance DRX-500 spectrometers. ^{1}H, ^{19}F and ^{13}C NMR spectra were recorded using the deuterated solvent as the lock and the residual solvent as the internal reference. The multiplicities of the spectroscopic data are presented in the following manner: s = singlet, bs = broad singlet, d = doublet, dd = double doublet, ddd = doublet of double doublets, dt = doublet of triplets, qd = quartet of doublets, t = triplet, tt = triplet of triplets and m = multiplet. Homocouplings (H–H, H–F, C–F) are given in Hertz and specified by J; the nuclei involved in heteronuclear couplings are defined with the observed nucleus given first. Unless stated otherwise, all refer to ^{3}J couplings. HRMS measurements were obtained from Thermofisher LTQ Orbitrap XL at the Engineering and Physical Sciences Research Council National Mass Spectrometry Service Centre, Swansea. Elemental analysis was performed on a PerkinElmer 2400 CHN analyser. GC-MS spectra were obtained on an instrument fitted with a DB5-type column (30 m × 0.25 μm) running a 40–320 °C (70–320 °C for acetates) temperature program, ramp rate 20 °C min^{-1} with helium carrier gas flow at 1 cm^3 min^{-1}. Electrospray mass spectra were obtained on a Thermo Finnegan LCQ Duo mass spectrometer (spray voltage 4.5 kV, mobile phase methanol). Melting points were recorded on a Griffin apparatus using open capillaries. IR spectra were recorded as films on a Shimadzu spectrometer with a Pike MIRacle horizontal single reflection ATR attachment. Thin layer chromatography was performed on pre-coated aluminium-backed silica gel plates (silica gel 60 F_{254}, thickness 0.2 mm, Merck KGaA, Darmstadt). Visualisation was achieved using vanillin or anisaldehyde staining and UV detection at 254 and 356 nm. Semi-automated column chromatography was performed on silica gel (Zeoprep 60 HYD, 40–63 μm, Zeochem) using a Büchi Sepacore system. Hexane was distilled before chromatography. Tetrahydrofuran and diethyl ether (for thioamide synthesis) were dried using a PureSolv system from Innovative Technology, Inc. Dimethyl carbonate was used as obtained from a chemical supplier. Microwave reactions were carried out in sealed vials in a Biotage Initiator 2.5.

Typical procedure: **Preparation of 8a**: Oxetan-3-one (0.68 mL, 10.6 mmol) followed by trifluoroacetic acid (0.40 mL, 5 mmol) were added to a solution of benzamide (1.21 g, 10 mmol) in acetic acid (20 mL). The colourless solution was heated to 120 °C for 3.5 h in a microwave reactor, then allowed to cool to room temperature. After venting and opening the vial, the black reaction mixture was concentrated under reduced pressure to remove any residual acid. The residue was treated with toluene (10 mL) then evaporated to afford crude product as a black tar (2.29 g). The crude product was taken up in a minimum volume of ethyl acetate (20 mL) and evaporated onto silica gel (1.5 g). The silica gel was made into a pad in a sinter funnel and washed with diethyl ether (250 mL). The washings were concentrated under reduced pressure to afford crude product as an orange/brown oil (2.1 g). Purification by column chromatography over silica gel (gradient 1:2 to 1:1 diethyl ether/hexane) afforded 2-phenyl 4-(acetoxymethyl)-oxazole (**8a**) as a colourless solid (932 mg, 47 %); R_f = 0.36 (2:5 diethyl ether/hexane); m.p. 39–40 °C (lit. m.p. 39.5–40 °C);[33] ^{1}H NMR (400 MHz, $CDCl_3$): δ = 8.08–8.05 (m, 2H; Ar*H*), 7.74 (s, 1H; H_5), 7.49–7.46 (m, 3H; Ar*H*), 5.12 (d, ^{4}J = 0.7 Hz, 2H; CH_2OAc), 2.13 ppm (s, 3H; CH_3); ^{13}C NMR (100 MHz, $CDCl_3$): δ = 170.3, 161.7, 136.7, 136.6, 130.1, 128.3, 126.7, 126.0, 57.6, 20.4 ppm; IR (film): $\tilde{\nu}$ = 1735, 1554, 1383, 1449, 1382, 1362, 1343, 1229 cm^{-1}; MS (CI): *m/z* (%): 258 (6) $[M+C_2H_5]^+$, 246 (10), $[M+C_2H_5]^+$, 218 (22) $[M+H]^+$, 174 (11) $[M-Ac]$, 158 (100) $[M-OAc]$, 104 (12); HRMS (ES-TOF): *m/z* calcd for $C_{12}H_{12}NO_3$: 218.0812 $[M+H]^+$; found: 218.0806; t_R (GC) = 12.20 min.

Typical procedure: **Preparation of 10a**: Oxetan-3-one (0.13 mL, 2 mmol) followed by methanesulfonic acid (65 μL, 1 mmol) were added to a suspension of benzamide (245 mg, 2.0 mmol) in dimethyl carbonate (4 mL). The reaction mixture was heated in a microwave reactor at 120 °C for 80 min; TLC confirmed full conversion. The reaction mixture was loaded onto a dry pad of celite (7.6 g), which was washed with dichloromethane

(125 mL). The filtrate was concentrated under reduced pressure and purified by column chromatography on silica gel (2:3 to 1:1 gradient of ethyl acetate in hexane) to afford 2-phenyl-4-(hydroxymethyl)-oxazole (**10a**) as a light brown solid (125 mg, 36%); $R_f = 0.25$ (1:1 ethyl acetate/hexane); m.p. 80–81 °C (lit. m.p. 82–83 °C);[32] ^{1}H NMR (400 MHz, $CDCl_3$): $\delta = 8.08$–8.05 (m, 2H; Ar*H*), 7.68 (s, 1H; H_5), 7.49–7.47 (m, 3H; Ar*H*), 4.71 (d, $J = 4.6$ Hz, 2H; ArCH_2OH); 2.26 ppm (brs, 1H; CH_2O*H*); ^{13}C NMR (100 MHz, $CDCl_3$): $\delta = 161.7$, 141.1, 134.5, 130.0, 128.3, 126.8, 126.0, 58.4 ppm; IR (film): $\tilde{\nu} = 3221$, 3116, 1740, 1552, 1351, 1231, 1023 cm^{-1}; MS (CI): *m/z* (%): 216 (7) $[M+C_3H_5]^+$, 204 (13) $[M+C_2H_5]^+$, 176 (40) $[M+H]^+$, 158 (100) $[M-OH]^+$), 130 (5); HRMS (ESI): *m/z* calcd for $C_{10}H_{10}NO_2$: 176.0706 $[M+H]^+$; found: 176.0705; t_R (GC) = 12.71 min. Crystal data for $C_{10}H_9NO_2$: Formula weight: 175.18; Temperature: 123(2) K; $\lambda = 0.71073$ Å; Monoclinic system; Crystal size: $0.24 \times 0.18 \times 0.10$ mm^3; Unit cell dimensions: $a = 8.5610(5)$, $b = 14.5900(8)$, $c = 7.0504(4)$ Å, $\alpha = 90$, $b = 104.625(6)$, $\gamma = 90°$; $Z = 4$; Reflection collected: 3925; *R* indices (all data): $R1 = 0.0647$, $wR2 = 0.1033$.

Typical procedure: **Preparation of 7f**: 4-Methoxybenzamide (376 mg, 2.5 mmol) was added to a suspension of P_2S_5/alumina reagent (773 mg, 3.5 mmol) in anhydrous THF (5 mL) and the reaction mixture was heated in a microwave reactor at 60 °C for 20 min until TLC showed complete conversion. The reaction mixture was evaporated onto a pad of silica gel (8.6 g), eluted with diethyl ether (50 mL), and the eluent was concentrated under reduced pressure to afford crude thioamide **7f** as a yellow solid (660 mg). The crude product was taken up in anhydrous THF (4 mL) and evaporated onto silica gel (2.6 g). The solid was transferred onto a pad of silica (10.6 g) in a sinter funnel that had been conditioned with 1:1 diethyl ether/hexane. Non-polar impurities were removed using 1:1 diethyl ether/hexane and product was eluted with 4:1 diethyl ether/hexane to afforded 4-(methoxy)thiobenzamide **7f** as a yellow solid (280 mg, 67%); $R_f = 0.23$ (4:1 diethyl ether/hexane); m.p. 141–143 °C; ^{1}H NMR (400 MHz, $CDCl_3$): $\delta = 7.92$–7.88 (m, 2H; one half of an AA′BB′ system, Ar*H*), 7.48 (brs, 1H; C(S)NH_aH$_b$), 7.09 (brs, 1H; C(S)N$H_a$$H_b$), 6.92–6.88 (m, 2H; one half of an AA′BB′ system Ar*H*), 3.86 ppm (s, 3H; ArOCH_3); ^{13}C NMR (100 MHz, $CDCl_3$): $\delta = 201.4$, 163.0, 131.3, 129.1, 113.6, 55.6 ppm; IR (film): $\tilde{\nu} = 3367$, 3278, 3157, 2363, 1626, 1597, 1510, 1427, 1389, 1330, 1285, 1258, 1184, 1138, 1020 cm^{-1}; MS (ESI): *m/z* (%): 168 (100) $[M+H]^+$, 151 (30) $[M-NH_2]$, 135 (15). The spectroscopic data were in agreement with those reported in the literature.[16a]

Computational methods: Electronic structure calculations were carried out on a Dell Precision T1500 (Intel 4 Core i7 CPU 870@ 2.93 GHz Processor, 8 GB RAM) running Spartan'08 V1.2.0, 64 Bit. Transition structures were located via initial guesses that were optimised using the PM3 semi-empirical method, then re-optimised initially at the RI-MP2/6-31G* or B3LYP/6-31G* levels of theory. These structures were then used as the starting points for MP2/6-31+G*or B3LYP/6-311+G** optimisations with full frequency calculation at 298 K. Free energies were evaluated (in au) using Spartan's internal algorithm and transferred to Excel for further manipulation. Optimised structures had no imaginary frequencies; unique imaginary frequencies were found for transition structures and these are listed fully with the Cartesian coordinates in the Supporting Information.

Acknowledgements

We thank EPSRC and GSK (Industrial CASE studentship to A.T.), GSK and the University of Strathclyde (studentship to D. O.), GSK Refractory Respiratory Inflammation DPU for consumables, the EPSRC National Mass Spectrometry Service Centre, Swansea for accurate mass measurements, Dr Alan Kennedy (Pure and Applied Chemistry, University of Strathclyde) for the X-ray structural determination of **10a**, Dr. Rob Young (GSK Stevenage) for helpful discussions about work-up methods, and David Black (University of Strathclyde) for preliminary syntheses of oxazoles **10**.

[1] G. Wuitschik, E. M. Carreira, B. Wagner, H. Fischer, I. Parrilla, F. Schuler, M. Rogers-Evans, K. Muller, *J. Med. Chem.* **2010**, *53*, 3227–3246.
[2] a) L. W. Ye, W. M. He, L. M. Zhang, *J. Am. Chem. Soc.* **2010**, *132*, 8550–8551; b) B. O. Beasley, G. J. Clarkson, M. Shipman, *Tetrahedron Lett.* **2012**, *53*, 2951–2953.
[3] a) M. A. J. Duncton, M. A. Estiarte, D. Tan, C. Kaub, D. J. R. O'Mahony, R. J. Johnson, M. Cox, W. T. Edwards, M. Wan, J. Kincaid, M. G. Kelly, *Org. Lett.* **2008**, *10*, 3259–3262; b) M. A. J. Duncton, M. A. Estiarte, R. J. Johnson, M. Cox, D. J. R. O'Mahony, W. T. Edwards, M. G. Kelly, *J. Org. Chem.* **2009**, *74*, 6354–6357.
[4] J. A. Burkhard, B. H. Tchitchanov, E. M. Carreira, *Angew. Chem.* **2011**, *123*, 5491–5494; *Angew. Chem. Int. Ed.* **2011**, *50*, 5379–5382.
[5] T. A. Mukhtar, G. D. Wright, *Chem. Rev.* **2005**, *105*, 529–542.
[6] F. Batt, F. Fache, *Eur. J. Org. Chem.* **2011**, 6039–6055.
[7] P. Wipf, *Chem. Rev.* **1995**, *95*, 2115–2134.
[8] a) R. Martín, A. Cuenca, S. L. Buchwald, *Org. Lett.* **2007**, *9*, 5521–5524; b) E. F. Flegeau, M. E. Popkin, M. F. Greaney, *Org. Lett.* **2008**, *10*, 2717–2720; c) S. A. Ohnmacht, P. Mamone, A. J. Culshaw, M. F. Greaney, *Chem. Commun.* **2008**, 1241–1243; d) C. K. Skepper, T. Quach, T. F. Molinski, *J. Am. Chem. Soc.* **2010**, *132*, 10286–10292; e) C. M. Counceller, C. C. Eichman, N. Proust, J. P. Stambuli, *Adv. Synth. Catal.* **2011**, *353*, 79–83; f) I. Cano, E. Alvares, M. C. Nicasio, P. J. Perez, *J. Am. Chem. Soc.* **2011**, *133*, 191–193; g) C. L. Paradise, P. R. Sarkar, M. Razzak, J. K. De Brabander, *Org. Biomol. Chem.* **2011**, *9*, 4017–4020; h) G. Bartoli, C. Cimarelli, R. Cipolletti, S. Diomedi, R. Giovannini, M. Mari, L. Marsili, E. Marcantoni, *Eur. J. Org. Chem.* **2012**, 630–636; i) A. E. Wendlandt, S. S. Stahl, *Org. Biomol. Chem.* **2012**, *10*, 3866–3870.
[9] R. K. Henderson, C. Jimenez-Gonzalez, D. J. C. Constable, S. R. Alston, G. G. A. Inglis, G. Fisher, J. Sherwood, S. P. Binks, A. D. Curzons, *Green Chem.* **2011**, *13*, 854–862.
[10] T. Durand-Reville, L. B. Gobbi, B. L. Gray, S. V. Ley, J. S. Scott, *Org. Lett.* **2002**, *4*, 3847–3850.
[11] M. L. P. Le, L. Cointeaux, P. Strobel, J. C. Lepretre, P. Judeinstein, F. Alloin, *J. Phys. Chem. C* **2012**, *116*, 7712–7718.
[12] a) C. Gabriel, S. Gabriel, E. H. Grant, B. S. J. Halstead, D. M. P. Mingos, *Chem. Soc. Rev.* **1998**, *27*, 213–223; b) P. Lidström, J. Tierney, B. Wathey, J. Westman, *Tetrahedron* **2001**, *57*, 9225–9283.
[13] a) H. Bilel, N. Hamdi, F. Zagrouba, C. Fischmeister, C. Bruneau, *Green Chem.* **2011**, *13*, 1448–1452; b) X. W. Miao, C. Fischmeister, C. Bruneau, P. H. Dixneuf, *ChemSusChem* **2008**, *1*, 813–816.
[14] a) C. M. Hou, Y. F. Chen, W. Li, *Carbohydr. Res.* **2012**, *355*, 87–91; b) U. Tilstam, *Org. Process Res. Dev.* **2012**, *16*, 1150–1153.
[15] a) J. P. Guthrie, *Can. J. Chem.* **1978**, *56*, 2342–2354; b) J. F. J. Dippy, S. R. C. Hughes, A. Rozanski, *J. Chem. Soc.* **1959**, 2492–2498; c) J. P. Candlin, R. G. Wilkins, *J. Chem. Soc.* **1960**, 4236–4241; d) W. P. Jencks, J. Regenstein in *Handbook of Biochemistry and Molecular Biology* (Ed.: G. D. Fasman), CRC, Boca Raton, **1976**, pp. 305–351.
[16] For syntheses of thioamides from nitriles, see: a) P. Y. Lin, W. S. Ku, M. J. Shiao, *Synthesis* **1992**, 1219–1220; b) M. C. Bagley, K. Chapaneri, C. Glover, E. A. Merritt, *Synlett* **2004**, 2615–2617; c) M. Nagl, C. Panuschka, A. Barta, W. Schmid, *Synthesis* **2008**, 4012–4018.
[17] H. R. Lagiakos, A. Walker, M. I. Aguilar, P. Perlmutter, *Tetrahedron Lett.* **2011**, *52*, 5131–5132.
[18] a) P. Ratcliffe, J. M. Adam, J. Baker, R. Bursi, R. Campbell, J. K. Clark, J. E. Cottney, M. Deehan, A. M. Easson, D. Ecker, D. Edwards, O. Epemolu, L. Evans, R. Fields, S. Francis, P. Harradine, F. Jeremiah, T. Kiyoi, D. McArthur, A. Morrison, P. Passier, J. Pick, P. G. Schnabel, J. Schulz, H. Steinbrede, G. Walker, P. Westwood, G. Wishart, J. U. de Haes, *Bioorg. Med. Chem. Lett.* **2011**, *21*, 2541–2546; b) M. Rega, P. Candal, C. Jimenez, J. Rodriguez, *Eur. J. Org. Chem.* **2007**, 934–942; c) R. Uy, L. Q. Yang, H. X. Zhou, S. C. Price, W. You, *Macromolecules* **2011**, *44*, 9146–9154.
[19] a) Z. Y. Li, L. Ma, J. Y. Xu, L. Y. Kong, X. M. Wu, H. Q. Yao, *Chem. Commun.* **2012**, *48*, 3763–3765; b) B. Di Credico, G. Reginato, L. Gonsalvi, M. Peruzzini, A. Rossin, *Tetrahedron* **2011**, *67*, 267–

274; c) H. Sugiyama, F. Yokokawa, T. Shioiri, *Org. Lett.* **2000**, *2*, 2149–2152.
[20] D. Sellanes, F. Campot, I. Nunez, G. Lin, P. Esposito, S. Dematteis, J. Saldana, L. Dominguez, E. Manta, G. Serra, *Tetrahedron* **2010**, *66*, 5384–5395.
[21] M. Yamaguchi, Y. Nobayashi, I. Hirao, *Tetrahedron Lett.* **1983**, *24*, 5121–5122.
[22] C. J. M. Stirling, *Tetrahedron* **1985**, *41*, 1613–1666.
[23] H. D. Banks, *Org. Biomol. Chem.* **2009**, *7*, 4496–4501.
[24] Spartan '08, Wavefunction, Irvine, CA, **2008**.
[25] L. Simón, J. M. Goodman, *Org. Biomol. Chem.* **2011**, *9*, 689–700.
[26] S. E. Wheeler, K. N. Houk, *J. Chem. Theory Comput.* **2010**, *6*, 395–404.
[27] a) J. B. Conant, W. R. Kirner, R. E. Hussey, *J. Am. Chem. Soc.* **1925**, *47*, 488–501; for examples in which adjacent unsaturation has little or no effect on the rate of nucleophilic substitution at sp^3 carbon, see b) D. N. Kevill, C. B. Kim, *J. Org. Chem.* **2005**, *70*, 1490–1493.
[28] For detailed MO treatments of the effect of adjacent unsaturation on nucleophilic substitution at sp^3 carbon, see a) D. Kost, K. Aviram, *J. Am. Chem. Soc.* **1986**, *108*, 2006–2013; b) R. E. Rawlings, A. K. McKerlie, D. J. Bates, Y. R. Mo, J. M. Karty, *Eur. J. Org. Chem.* **2012**, 5991–6004.
[29] A. Noel, B. Delpech, D. Crich, *Org. Biomol. Chem.* **2012**, *10*, 6480–6483.
[30] A reviewer pointed out that the usual ideal gas equation penalises bimolecular reactions entropically at the expense of unimolecular reactions, and that termolecular reactions may suffer a still more severe penalty; for QM calculations on termolecular reaction steps, see a) S. K. Ignatov, P. G. Sennikov, A. G. Razuvaev, O. Schrems, *J. Phys. Chem. A* **2004**, *108*, 3642–3649; b) M. Ismael, R. Sahnoun, A. Suzuki, M. Koyama, H. Tsuboi, N. Hatakeyama, A. Endou, H. Takaba, M. Kubo, S. Shimizu, C. A. Del Carpio, A. Miyamoto, *Int. J. Greenhouse Gas Control* **2009**, *3*, 612–616; c) H. Yamada, Y. Matsuzaki, T. Higashii, S. Kazama, *J. Phys. Chem. A* **2011**, *115*, 3079–3086; d) M. Torrent-Sucarrat, J. S. Francisco, J. M. Anglada, *J. Am. Chem. Soc.* **2012**, *134*, 20632–20644; for an approach to the evaluation of Gibbs energy barriers for reactions of higher molecularity, see D. Ardura, R. Lopez, T. L. Sordo, *J. Phys. Chem. B* **2005**, *109*, 23618–23623.
[31] a) A. C. Chamberlin, C. J. Cramer, D. G. Truhlar, *J. Phys. Chem. B* **2008**, *112*, 8651–8655; b) C. J. Cramer, D. G. Truhlar, *Acc. Chem. Res.* **2008**, *41*, 760–768.
[32] a) W. P. Jencks, *Chem. Rev.* **1972**, *72*, 705–718; b) R. A. O'Ferrall, *J. Chem. Soc. B* **1970**, 274–277.
[33] A. B. A. Jansen, M. Szelke, *J. Chem. Soc.* **1961**, 405–411.

Received: March 16, 2013
Published online: ■■ ▮▮, 0000

Open sesame: The direct microwave-mediated condensation between 3-oxetanone and primary amides and thioamides has delivered moderate to good yields of oxazoles and thiazoles. The reactions use a sustainable solvent, require only short reaction times and represent a highly competitive method for the construction of two classes of valuable heteroarenes. Electronic structure calculations have been used to probe a range of potential reaction mechanisms (see figure).

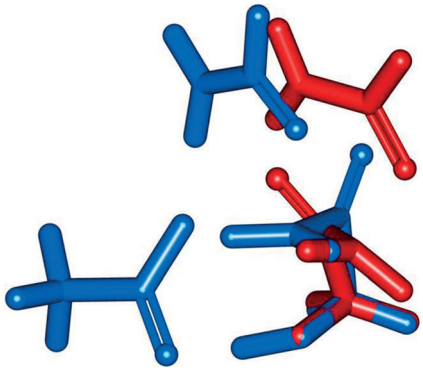

Heterocyclic Synthesis

D. Orr, A. Tolfrey, J. M. Percy, J. Frieman, Z. A. Harrison,* M. Campbell-Crawford, V. K. Patel* ..... ▮▮▮▮–▮▮▮▮

Single-Step Microwave-Mediated Syntheses of Oxazoles and Thiazoles from 3-Oxetanone: A Synthetic and Computational Study